

Anti-parity-time symmetric phase transition in diffusive systems

Pei-Chao Cao(曹培超) and Xue-Feng Zhu(祝雪丰)

Citation: Chin. Phys. B, 2021, 30 (**3**): 030505. DOI: 10.1088/1674-1056/abd694
Journal homepage: http://cpb.iphy.ac.cn; http://iopscience.iop.org/cpb

What follows is a list of articles you may be interested in

Dynamic phase transition of ferroelectric nanotube described by a spin-1/2 transverse Ising model

Chundong Wang(王春栋), Ying Wu(吴瑛), Yulin Cao(曹喻霖), and Xinying Xue(薛新英)
Chin. Phys. B, 2021, 30 (**2**): 020504. DOI: 10.1088/1674-1056/abbbfd

Quantum quenches in the Dicke model: Thermalization and failure of the generalized Gibbs ensemble

Xiao-Qiang Su(苏晓强) and You-Quan Zhao(赵有权)
Chin. Phys. B, 2020, 29 (**12**): 120506. DOI: 10.1088/1674-1056/abc679

Fast and accurate determination of phase transition temperature via individual generalized canonical ensemble simulation

Ming-Zhe Shao(邵明哲), Yan-Ting Wang(王延颋), Xin Zhou(周昕)
Chin. Phys. B, 2020, 29 (**8**): 080505. DOI: 10.1088/1674-1056/ab9c03

Topological Anderson insulator in two-dimensional non-Hermitian systems

Hongfang Liu(刘宏芳), Zixian Su(苏子贤), Zhi-Qiang Zhang(张智强), Hua Jiang(江华)
Chin. Phys. B, 2020, 29 (**5**): 050502. DOI: 10.1088/1674-1056/ab8201

Entangled multi-knot lattice model of anyon current

Tieyan Si(司铁岩)
Chin. Phys. B, 2019, 28 (**4**): 040501. DOI: 10.1088/1674-1056/28/4/040501

TOPICAL REVIEW — Phononics and phonon engineering

Anti-parity-time symmetric phase transition in diffusive systems*

Pei-Chao Cao(曹培超) and Xue-Feng Zhu(祝雪丰)†

School of Physics and Innovation Institute, Huazhong University of Science and Technology, Wuhan 430074, *China*

(Received 27 September 2020; revised manuscript received 2 December 2020; accepted manuscript online 24 December 2020)

Parity-time (PT) symmetry/anti-parity-time (APT) symmetry in non-Hermitian systems reveal profound physics and spawn intriguing effects. Recently, it has been introduced into diffusive systems together with the concept of exceptional points (EPs) from quantum mechanics and the wave systems. With the aid of convection, we can generate complex thermal conductivity and imitate various wavelike dynamics in heat transfer, where heat flow can be "stopped" or moving against the background motion. Non-Hermitian diffusive systems offer us a new platform to investigate the heat wave manipulation. In this review, we first introduce the construction of APT symmetry in a simple double-channel toy model. Then we show the phase transition around the EP. Finally, we extend the double-channel model to the four-channel one for showing the high-order EP and the associated phase transition. In a general conclusion, the phase difference of adjacent channels is always static in the APT symmetric phase, while it dynamically evolves or oscillates when the APT symmetry is broken.

Keywords: anti-parity-time symmetry, phase transition, exceptional point, heat transfer

PACS: 05.70.fh, 44.10.+i **DOI:** 10.1088/1674-1056/abd694

1. Introduction

In quantum mechanics, Hermitian Hamiltonians are widely used in describing the closed systems with orthogonal eigenstates and real eigenvalues. While in open systems, such as wave systems with gain or loss, the corresponding Hamiltonians are typically non-Hermitian with non-orthogonal eigenstates and complex eigenvalues, which brings challenges to evaluate the systems experimentally.[1] Until 1998, Bender and Boettcher discovered that systems exhibiting parity-time (PT) symmetry, subjected to $[PT, H] = 0$, could display entirely real spectra below some threshold.[2] The threshold is later termed as an exceptional point (EP), where the eigenvalues and eigenvectors of H are degenerated, corresponding to mode generation or annihilation in parameter space.[3,4] Starting with the similarity between the quantum Schrödinger equation and paraxial wave equation, PT symmetry can be constructed in analogy by incorporating balanced gain and loss materials.[5] Various counterintuitive phenomena or nontrivial effects are theoretically and experimentally proposed in this new platform, such as one-way mode conversion,[6–10] coherent lasing and absorption,[11–13] EP-based sensing,[14–16] mode switches,[17,18] and topological bound states.[19–21]

As a counterpart, anti-PT symmetry, subjected to $\{PT, H\} = 0$, was first proposed by replacing the balanced gain and loss with positive and negative refractions.[22] Subsequent theoretical and experimental realizations were conducted in different fields, ranging from cold-atom systems, nonlinear wave systems to the effective dissipative coupling systems.[23–28] In a mathematical view, the equivalent dissipative coupling always induces the APT symmetric Hamiltonian $H_{\rm APT}$, which just is the result of PT symmetric Hamiltonian $H_{\rm PT}$ by multiplied with an imaginary number i.[24,26] Since the APT symmetry is the complex conjugate of the PT symmetry, the corresponding phase transitions in those systems display two polar-opposite evolution paths in physics.

The APT symmetry was firstly introduced into diffusive systems by the analogy of wave equation and convection-diffusion equation in the past year.[29] In fact, there exist precedents for the wave-diffusion mapping, which has advanced successes. A classical example is the functional heat manipulation via metamaterials designed by coordinate transformation theory,[30,31] such as thermal cloaks,[32–34] thermal camouflages and illusion,[35,36] and other thermal managements,[37,38] which also has a counterpart in electromagnetic and acoustic fields. Back to the APT symmetry in diffusive systems, it should be noticed that the heat transfer is a natural diffusion process. Thus the coupling between different channels or materials is spontaneously imaginary. Compared with the wave systems, through mimicking the pulse transport with convection flows, we can generate a similar wavelike transmission in diffusive systems.[29,39] Details can be found in the following.

*Project supported by the National Natural Science Foundation of China (Grant Nos. 11674119 and 11690032) and the Fundamental Research Funds for the Central Universities, China (HUST: 2019JYCXJJ038). X. F. Z. and P. C. C. acknowledge the financial support from the Bird Nest Plan of HUST.

†Corresponding author. E-mail: xfzhu@hust.edu.cn

© 2021 Chinese Physical Society and IOP Publishing Ltd

2. The realization of APT symmetry in diffusive systems

2.1. Theoretical background: PT/APT symmetry and EP in wave systems

As there exists energy exchange with environment, Hamiltonian in non-Hermitian systems displays the relation $H \neq H^{\dagger}$ (transposition plus complex conjugation). Thus, the conservativeness of measuring a particle's property with unitary time evolution is broken, or the complex energy eigenvalues principally make the systems unstable and unobservable. However, Bender and Boettcher showed that a non-Hermitian system satisfying $[PT, H] = PTH - HPT = 0$ can obtain purely real eigenvalues,[2] where P is the parity symmetry operator (a system at P symmetry is equivalent to its mirror image) and T is the time symmetry operator (a system at T symmetry returns to the original state, when the time goes backward). Intuitively, a second-order Hamiltonian satisfying PT symmetry[40,41]

$$H_{\mathrm{PT}} = \begin{pmatrix} \omega_0 + \mathrm{i}g & \kappa \\ \kappa & \omega_0 - \mathrm{i}g \end{pmatrix} \tag{1}$$

describes a double-channel non-Hermitian system with complex frequencies $\omega_0 \pm \mathrm{i}g$, where g is a positive number with the sign '$\pm$' being a gain/loss coefficient, and κ is the coupling strength, as shown in Fig. 1(a).[40] The eigenvalues and eigenvectors can be obtained as

$$\omega_{\mathrm{PT}\pm} = \omega_0 \pm \sqrt{\kappa^2 - g^2}. \tag{2}$$

However, a Hamiltonian satisfying APT symmetry $\{PT, H\} = PTH + HPT = 0$ has a different form[22,24,26]

$$H_{\mathrm{APT}} = \begin{pmatrix} \omega_0 + \mathrm{i}g & \mathrm{i}\kappa \\ \mathrm{i}\kappa & -\omega_0 + \mathrm{i}g \end{pmatrix}, \tag{3}$$

with the real part of the complex frequencies in opposite sign and the imaginary part being the same. The coupling coefficient between different components is purely imaginary, as shown in Fig. 1(b), which however is not easy to realize in experiments. Then the eigenvalues and eigenvectors of H_{APT} can be obtained as follows:

$$\omega_{\mathrm{APT}\pm} = \mathrm{i}\left(g \pm \sqrt{\kappa^2 - \omega_0^2}\right). \tag{4}$$

Figures 1(a) and 1(b) show the schematic of how to construct PT symmetry and APT symmetry in wave systems. PT symmetry can be usually realized in a structure with balanced gain and loss distribution. Due to the difficulty of doping gain materials, the weak form of passive PT, with complex frequencies of the systems produced by different loss rates, has attracted lots of attention. In general, dissipation is regarded as a major negative factor especially in long-distance wave transport and processing. However, with the aid of PT symmetry theory, a structure with some losses can still produce high-quality single mode lasing.[40] Compared with PT symmetry system, the APT symmetry system cannot go back to its original state after an odd number of PT symmetry operations, and phase transition in the APT symmetry system shows an opposite state evolution.

As shown in Eqs. (2) and (4), there exists a critical point (EP), where both real and imaginary parts of eigenvalues are degenerate, as marked by the green stars in Fig. 2. It is shown that the eigenvalues of the PT symmetry system change from real (complex) to complex (real) after crossing the EP, while the eigenvalues of the APT symmetry system change from imaginary (complex) to complex (imaginary) after crossing the EP. In the symmetric phase, PT symmetry system and APT symmetry system are featured with uniformly distributed amplitudes and steady phase differences in the coupling channels, respectively. In the symmetry broken phase, PT symmetry system and APT symmetry system are featured with unequally distributed amplitudes and transient evolving phases, respectively.

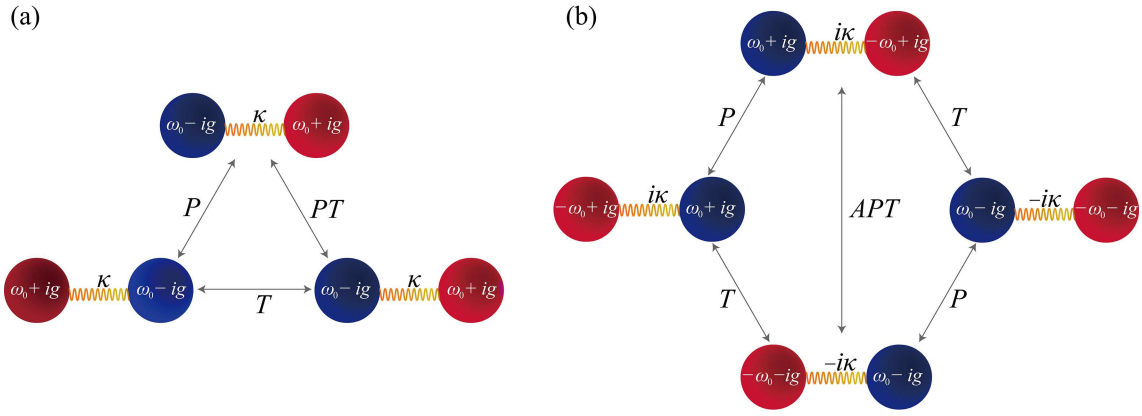


Fig. 1. The realization of PT symmetry and APT symmetry in wave systems. The parity operator (P) exchanges the spatial coordinates and the time operator (T) takes the conjugation of complex parameters (gain, loss, or coupling strength). (a) PT symmetry can be constructed by a system of two coupled structures with balanced gain $(+\mathrm{i}g)$ and loss $(-\mathrm{i}g)$, and the coupling strength (κ) is always real. (b) APT symmetry can be constructed by a system of two coupled structures with opposite real frequencies (positive and negative refractive indices), and the coupling strength is imaginary $(\mathrm{i}\kappa)$.

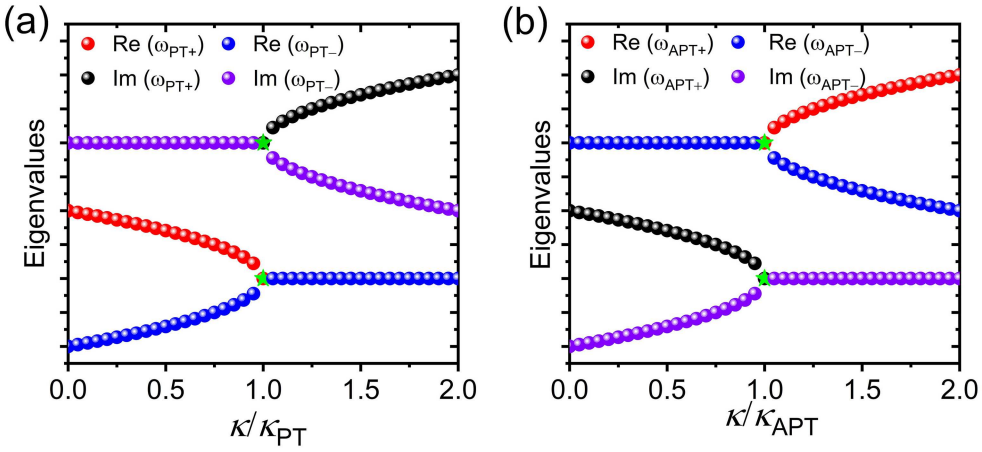


Fig. 2. The eigenvalues of (a) PT symmetry systems and (b) APT symmetry systems versus the coupling strength κ. EPs are marked by the green stars.

2.2. The realization of APT symmetry in diffusive systems

In the above analyses, the key point in the realization of APT symmetry is to construct an imaginary coupling between two systems. However, the coupling in non-dissipative waveguide systems is real due to the invariant essence of PT symmetry operator. Researchers have made great efforts to overcome these difficulties. In 2016, the first experimental demonstration of optical APT symmetry was realized by setting rapidly flying atoms between two long-lived atom spin waves, which can produce an effective dissipative coupling.[24] As a result, unidirectional reflectionless light transport was observed. In 2017, this method was introduced into waveguide coupling systems.[26] In 2018, dissipative coupling was implemented in a resistively coupled amplifying-*LRC*-resonator circuit.[27] In 2019, C. T. Chan *et al.* found that APT symmetric system can be employed for asymmetric mode switching, with an EP dynamically encircled.[28]

Different with wave systems, thermal system is an inherent dissipative one with energy exchange in an open environment. Thus, the coupling coefficient is imaginary spontaneously. Compared with the complicated post-processing in wave systems, APT symmetry can be realized in diffusive systems in a much easier way. In analogy with the positive and negative refraction indices in optics by introducing opposite convection flows in coupling diffusive systems, APT symmetry can be directly implemented (Fig. 3(a)).[29] Figure 3 shows the two paths to construct PT/APT symmetry in wave systems and diffusive systems. With the aid of convection-diffusion physical process, heat can be dynamically stopped, or even flows against the moving background. The simplest way is to bridge the two opposite rotating rings through a thermal coupling layer. As shown in Figs. 3(c) and 3(d), the parameters b and d are the thicknesses of the channels and the interlayer. R_1 and R_2 are the inner and outer radii ($R_1 \approx R_2$). v and Ω are the linear velocity and rotating angular velocity of the channels, respectively ($\Omega = v/R_1$).

3. Phase transition

According to the Fourier law, the temperature field of a convection-diffusion system is expressed as[42]

$$\rho C_p \frac{\partial T}{\partial t} = \kappa \frac{\partial^2 T}{\partial x^2} - \rho C_p v \frac{\partial T}{\partial x}, \tag{5}$$

where ρ, C_p, and κ are the density, heat capacity, and thermal conductivity of the material, and v is the velocity of the moving background. From Eq. (5), we can find when the coefficient of thermal diffusion term is very small, only the convection term dominates, and the convection flow of heat is just like the wave-packet transport. If we take the temperature profile in the wave form $T = T_0 + A\,\mathrm{e}^{\mathrm{i}(kx-\omega t)}$, where T_0 is the reference temperature and can be chosen as 0 for simplify, A is the temperature gradient, $k = 2\pi/L$ is the zero-order wave number, L is the length of the channel, and ω is the frequency. Submitting the wave form solution into Eq. (5), we can generate a complex frequency $\omega = -\mathrm{i}k^2 D + kv$ ($D = \frac{\kappa}{\rho C_p}$ is the diffusion coefficient) or an effective complex thermal conductivity.[33,43] In this way, the coupling equation of structures in Figs. 3(c) and 3(d) can be deduced as follows:[29,39]

$$\begin{aligned} \frac{\partial T_1}{\partial t} &= D\frac{\partial^2 T_1}{\partial x^2} - v\frac{\partial T_1}{\partial x} + \frac{h_{s+}}{\rho C_p}, \\ \frac{\partial T_2}{\partial t} &= D\frac{\partial^2 T_2}{\partial x^2} + v\frac{\partial T_2}{\partial x} + \frac{h_{s-}}{\rho C_p}, \end{aligned} \tag{6}$$

where $h_s = q/b$ can be regarded as a heat source from the channels to the interlayer boundaries. The source is uniformly distributed along the thickness direction. From the boundary matching conditions that temperature and heat flux are both continuous at the interfaces, we can deduce $h_{s+} = -\frac{k_i(T_1-T_2)}{bd}$ and $h_{s-} = \frac{k_i(T_1-T_2)}{bd}$, where k_i is the thermal conductivity of the interlayer.

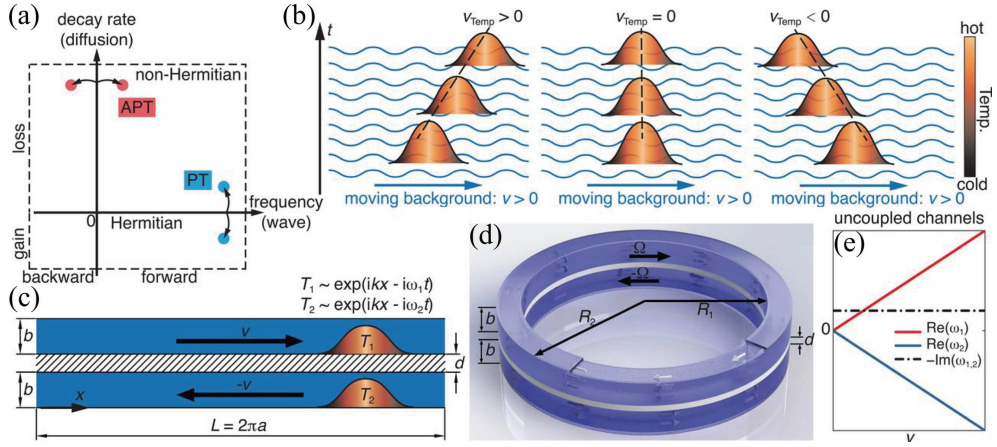


Fig. 3. The realization of APT symmetry in diffusive systems.[29] (a) PT symmetry can be constructed by balancing gain and loss in wave systems. APT symmetry can be constructed by opposite convection flows in diffusive systems. (b) Temperature profiles can follow, hold, or even move against the background motion with the convection flow modulation. (c) and (d) 2D and 3D models of APT symmetry systems. (e) Eigenvalues in the case of uncoupling.

3.1. APT symmetric phase

Based on Eq. (6), the Hamiltonian of this APT symmetric system is established[29]

$$H = \begin{pmatrix} -\mathrm{i}(k^2 D + h) + kv & \mathrm{i}h \\ \mathrm{i}h & -\mathrm{i}\left(k^2 D + h\right) - kv \end{pmatrix} \tag{7}$$

where $\mathrm{i}h = \mathrm{i}\frac{k_i}{\rho C_p bd}$ is the imaginary coupling coefficient or the energy exchange rate between channels. Solving Eq. (7) we can obtain the eigenfrequencies and eigenvectors as follows:

$$\begin{aligned} \omega_\pm &= -\mathrm{i}\left(S_0 \pm \sqrt{h^2 - k^2 v^2}\right), \\ u_\pm &= \left(kv/h \pm \mathrm{i}\sqrt{1-(kv/h)^2},\ \mathrm{i}\right)^{\mathrm{T}}, \end{aligned} \tag{8}$$

where $S_0 = k^2 D + h$. To generate the temperature profile exactly, we can combine the forward and backward solutions together as

$$(T_{1\pm}, T_{2\pm}) = \mathrm{e}^{-\mathrm{i}\omega_\pm t}\left[A\,\mathrm{e}^{\mathrm{i}kx} u_\pm(k) + B\,\mathrm{e}^{-\mathrm{i}kx} u_\pm(-k)\right]. \tag{9}$$

It is clearly shown that the EP in parameter space is at the threshold as v increases to $v_{\mathrm{EP}} = h/k$. When $v \le v_{\mathrm{EP}}$, the eigenfrequencies are pure imaginary and the eigenvectors in different channels have uniform modulus ($A = B = 1$). Moreover, the eigenvectors satisfy the symmetry relation $PTu_\pm = -u_\pm$, and the system is under the exact APT symmetric regime with a static phase difference of $\theta = \sin^{-1}(v/v_{\mathrm{EP}})$ and equal amplitudes in all channels. The temperature fields in different channels are

$$(T_{1\pm}, T_{2\pm}) = 2\,\mathrm{e}^{-\mathrm{i}\omega_\pm t}(\cos kx, \pm\cos(kx \pm \theta)). \tag{10}$$

3.2. APT symmetry broken phase

If the flow velocity is continually increased and surpasses the EP, $v > v_{\mathrm{EP}}$, the eigenfrequencies become complex and the moduli of different channels are unequal. APT symmetry is broken with a time-varying phase difference and nonuniform distribution amplitudes. To facilitate the calculation process, we take a parameter $\psi = \cosh - 1(v/v_{\mathrm{EP}})$ and extract the real part of the eigenfrequencies out. The temperature field can be expressed as[29]

$$\begin{aligned} T_j = \mathrm{e}^{\mathrm{Im}\omega_\pm t}\big[&A_j \cos(kx - \mathrm{Re}(\omega)t + \varphi_j) \\ &+ B_j \cos(kx + \mathrm{Re}(\omega)t + \varphi_j)\big], \end{aligned} \tag{11}$$

where $j = 1, 2, A_1 = AA_2 = A\,\mathrm{e}^{-\psi} B_1 = BB_2 = B\,\mathrm{e}^{\psi}$, and $\varphi_2 - \varphi_1 = \pi/2$. According to Eq. (11), the trajectory of the maximum points in the channels can be calculated as

$$\tan[kx_j(t) + \varphi_j] = \frac{\tan[\mathrm{Re}(\omega)t](A_j - B_j)}{A_j + B_j}$$

with a phase difference

$$\begin{aligned} \varphi(t) &= kx_1(t) - kx_2(t) \\ &= \varphi_0 + \tan^{-1}\frac{S_1 \tan[\mathrm{Re}(\omega)t]}{1 + S_2 \tan^2[\mathrm{Re}(\omega)t]}, \end{aligned} \tag{12}$$

where

$$S_1 = \frac{A_1 - B_1}{A_1 + B_1} - \frac{A_2 - B_2}{A_2 + B_2}, \quad S_2 = \frac{A_1 - B_1}{A_1 + B_1} \cdot \frac{A_2 - B_2}{A_2 + B_2}.$$

We take the material parameters as $\rho = 103$ kg/m^3, $C_p = 103$ J/(kg·K), $\kappa = 100$ W/(m·K), $\kappa_i = 1$ W/(m·K) and the structure parameters as $b = 5$ mm, $d = 1$ mm, $R_1 = 0.1$ m, $R_2 = 0.11$ m in the finite element solver COMSOL Multiphysics® 5.3. Then the coupling coefficient can be deduced as $h = 0.2$ s^{-1}, wave number $k = 10$ m^{-1}, and diffusion coefficient $D = 10^{-4}$ m^2/s. Figure 4 shows the transient phase transition with the convection flow velocity increasing from below v_{EP} to above v_{EP}, the initial conditions are $T = 293.15 + 0.5y$ and $T = 293.15 + 0.5x$, respectively.

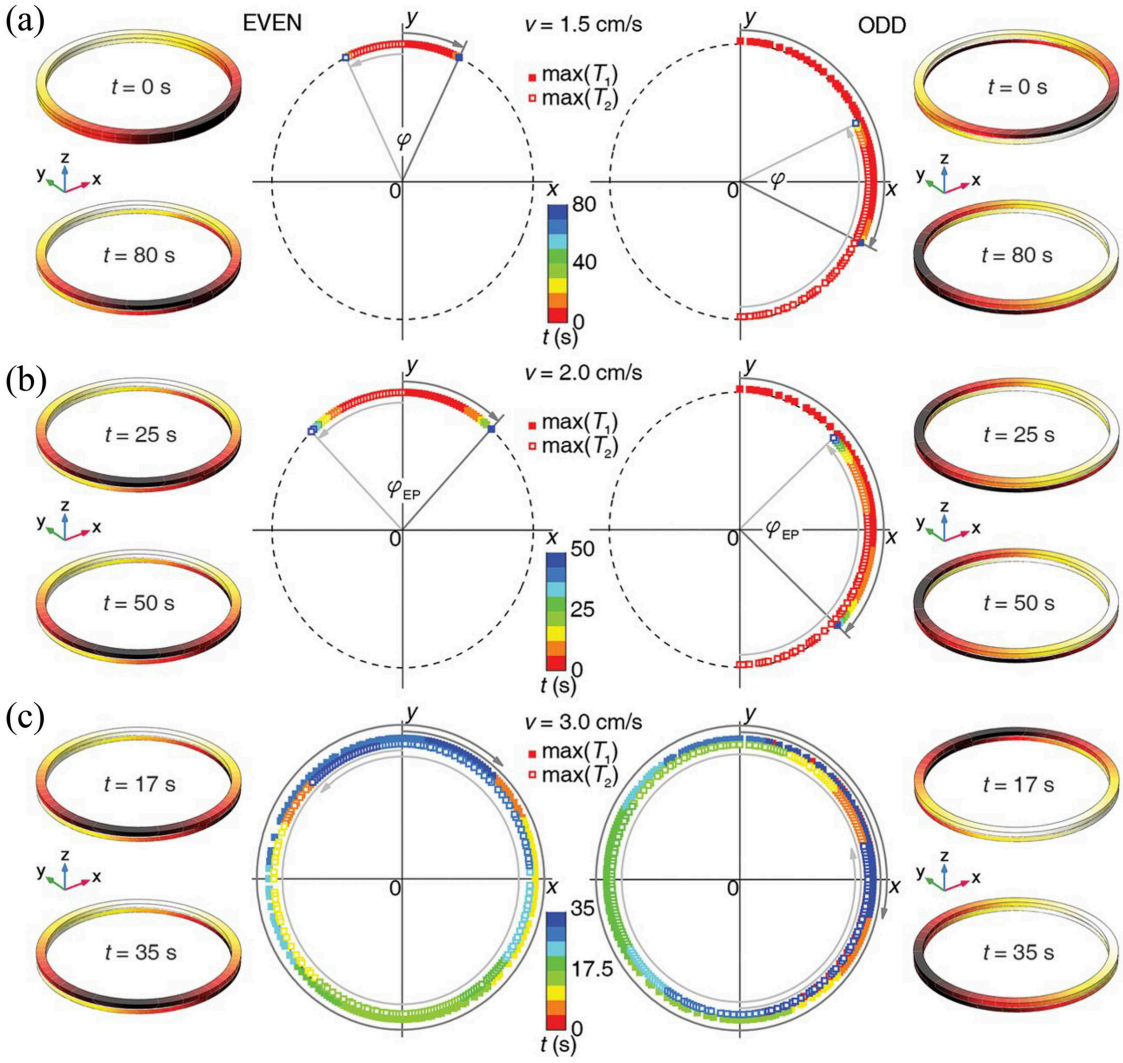


Fig. 4. Numerical calculation of transient phase evolution in the APT symmetric system.[29] (a) $v < v_{\rm EP}$. (b) $v = v_{\rm EP}$. (c) $v > v_{\rm EP}$.

3.3. Experiments

From above, we can predict the counterintuitive phenomenon of heat "stopping" with a static phase difference in the APT symmetry phase. When we increase the velocity of moving background at $v > v_{\rm EP}$, the temperature profile evolves in time. Going one step further, can we make the temperature profile move against the motion of background, or so-called negative thermal transport? In fact, if the channels are given different initial phases and temperature gradients, we can achieve a counter-flow of heat in the reverse direction.[29,43]

As shown in Fig. 3(d), we can use two oppositely rotating motors to drive the two rings in contact, where the grease is painted evenly between them. Initial temperature gradients can be imposed through a copper plate with one side in hot water bath and the other side in cold water bath.

4. High-order EP in diffusive systems

4.1. Phase transition at high-order EP

Compared with the double-channel toy model with one EP, previous works in wave systems inspire us that multiple channels can have higher-order EPs, which will be illustrated in the following. Figure 5(a) shows a four-channel convection-diffusion-coupling structure with adjacent channels at the same but opposite velocities. From Eqs. (5)–(7), we can deduce the Hamiltonian of this system as[39]

$$H = \begin{pmatrix} -\mathrm{i}S_0 - kv & \mathrm{i}h & 0 & 0 \\ \mathrm{i}h & -\mathrm{i}(S_0+h)+kv & \mathrm{i}h & 0 \\ 0 & \mathrm{i}h & -\mathrm{i}(S_0+h)-kv & \mathrm{i}h \\ 0 & 0 & \mathrm{i}h & -\mathrm{i}S_0+kv \end{pmatrix}. \tag{13}$$

The eigenvalues are solved, in Fig. 5(b), from which we find that there are two EPs, denoted by A and B, as marked by green

stars;

$$\omega_{\pm1} = -\mathrm{i}\left(S_0 \pm \sqrt{h^2 - k^2v^2}\right), \quad \omega_{\pm2} = -\mathrm{i}\left(S_0 + h \pm \sqrt{2h^2 - k^2v^2}\right). \tag{14}$$

The eigenvectors are also derived as follows:[39]

$$u_{\pm1} = \left(-\frac{-h^2 + 2k^2v^2 \pm 2\mathrm{i}kv\sqrt{h^2 - k^2v^2}}{h^2}, -\frac{-\mathrm{i}kv \pm \sqrt{h^2 - k^2v^2}}{h}, -\frac{-\mathrm{i}kv \pm \sqrt{h^2 - k^2v^2}}{h}, 1\right)^{\mathrm{T}},$$
$$u_{\pm2} = \left(-1, \frac{h + \mathrm{i}kv \pm \sqrt{2h^2 - k^2v^2}}{h}, -\frac{h - \mathrm{i}kv \pm \sqrt{2h^2 - k^2v^2}}{h}, 1\right)^{\mathrm{T}}. \tag{15}$$

Different from the double-channel toy model with only one second-order EP, we can obtain a third-order EP at A and the other second-order EP at B.

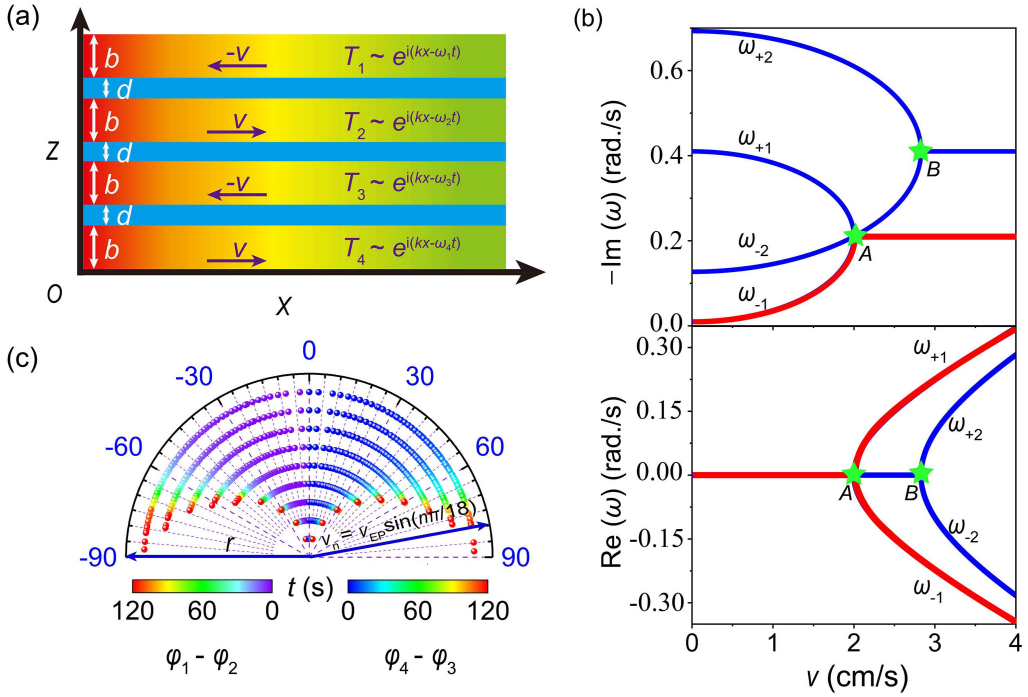


Fig. 5. (a) A schematic of the 2D model with high-order EP in diffusive systems.[39] (b) Eigenvalues evolve with convection flow velocity, the EPs are marked with green stars. (c) Transient phase differences of adjacent channels in APT symmetric phase.

We can calculate the higherorder EP with eigenvalues as $\omega_{\pm1,-2} = -\mathrm{i}S_0$, $\omega_{+2} = -\mathrm{i}(S_0 + 2h)$ and eigenvectors as $u_{\pm1,-2} = (-1, \mathrm{i}, \mathrm{i}, 1)^{\mathrm{T}}$, $u_{+2} = (-1, 2+\mathrm{i}, -2+\mathrm{i}, 1)^{\mathrm{T}}$ at $v_{\mathrm{EP1}} = h/k$. It shows that all the eigenvalues and eigenvectors are degenerate at the third-order EP. When it comes to the EP B ($v_{\mathrm{EP2}} = \sqrt{2}h/k$), the eigenvalues and eigenvectors are calculated to be $\omega_{\pm1} = -\mathrm{i}(S_0 \pm h)$, $\omega_{\pm2} = -\mathrm{i}(S_0 + h)$ and $u_{\pm1} = \left[-3 \pm 2\sqrt{2}, \mathrm{i}\left(\mp1 + \sqrt{2}\right), \mathrm{i}\left(\mp1 + \sqrt{2}\right), 1\right]^{\mathrm{T}}$, $u_{\pm2} = \left[-1, 1 + \mathrm{i}\sqrt{2}, -1 + \mathrm{i}\sqrt{2}, 1\right]^{\mathrm{T}}$ with only two eigenstates degenerated. It should be noted that the eigenstates in the diffusive systems evolve in the minimum-loss path, which is denoted by the red line in Fig. 5(b). In Fig. 5(c), we show the transient phase differences of adjacent channels below v_{EP1}, from which we find that all the phase differences are static after a time evolution. This is also illustrated from the temperature profile in theory as following:[39]

$$T_{+1} = 2\mathrm{e}^{-\mathrm{i}\omega_{+1}t}\left[\cos(kx - 2\vartheta), -\cos(kx - \vartheta), -\cos(kx - \vartheta), \cos kx\right]^{\mathrm{T}},$$
$$T_{-1} = 2\mathrm{e}^{-\mathrm{i}\omega_{-1}t}\left[\cos(kx + 2\vartheta), \cos(kx + \vartheta), \cos(kx + \vartheta), \cos kx\right]^{\mathrm{T}},$$
$$T_{+2} = 2\mathrm{e}^{-\mathrm{i}\omega_{+2}t}\left[-\cos kx, \left(1 + \sqrt{2 - \sin 2\vartheta}\right)\cos kx - \sin\vartheta \sin kx, -\left(1 + \sqrt{2 - \sin 2\vartheta}\right) - \sin\vartheta \sin kx, \cos kx\right]^{\mathrm{T}},$$
$$T_{-2} = 2\mathrm{e}^{-\mathrm{i}\omega_{+2}t}\left[-\cos kx, \left(1 - \sqrt{2 - \sin 2\vartheta}\right)\cos kx - \sin\vartheta \sin kx, -\left(1 - \sqrt{2 - \sin 2\vartheta}\right) - \sin\vartheta \sin kx, \cos kx\right]^{\mathrm{T}}, \tag{16}$$

where $\vartheta = \sin^{-1}(v/v_{\mathrm{EP1}})$. When $v > v_{\mathrm{EP1}}$, the APT symmetry is broken ($PTu_{\pm} \neq -u_{\pm}$). In the APT symmetry broken phase,

substituting $\psi = \cosh -1\,(v/v_{\rm EP})$ into Eq. (15), we can obtain[39]

$$T_{+1} = \mathrm{e}^{\mathrm{Im}(\omega_{+1})t}\begin{bmatrix} -\mathrm{e}^{-2\psi}\cos\left(kx-\mathrm{Re}\left(\omega_{+1}\right)t\right)-\mathrm{e}^{2\psi}\cos\left(kx+\mathrm{Re}\left(\omega_{+1}\right)t\right), \\ \mathrm{e}^{-\psi}\cos\left(kx-\mathrm{Re}\left(\omega_{+1}\right)t\right)+\mathrm{e}^{\psi}\cos\left(kx+\mathrm{Re}\left(\omega_{+1}\right)t\right), \\ \mathrm{e}^{-\psi}\cos\left(kx-\mathrm{Re}\left(\omega_{+1}\right)t\right)+\mathrm{e}^{\psi}\cos\left(kx+\mathrm{Re}\left(\omega_{+1}\right)t\right), \\ \cos\left(kx-\mathrm{Re}\left(\omega_{+1}\right)t\right)+\cos\left(kx+\mathrm{Re}\left(\omega_{+1}\right)t\right) \end{bmatrix}^{\mathrm{T}},$$

$$T_{-1} = \mathrm{e}^{\mathrm{Im}(\omega_{-1})t}\begin{bmatrix} -\mathrm{e}^{2\psi}\cos\left(kx-\mathrm{Re}\left(\omega_{-1}\right)t\right)-\mathrm{e}^{-2\psi}\cos\left(kx+\mathrm{Re}\left(\omega_{-1}\right)t\right), \\ \mathrm{e}^{\psi}\cos\left(kx-\mathrm{Re}\left(\omega_{-1}\right)t\right)+\mathrm{e}^{-\psi}\cos\left(kx+\mathrm{Re}\left(\omega_{-1}\right)t\right), \\ \mathrm{e}^{\psi}\cos\left(kx-\mathrm{Re}\left(\omega_{-1}\right)t\right)+\mathrm{e}^{-\psi}\cos\left(kx+\mathrm{Re}\left(\omega_{-1}\right)t\right), \\ \cos\left(kx-\mathrm{Re}\left(\omega_{-1}\right)t\right)+\cos\left(kx+\mathrm{Re}\left(\omega_{-1}\right)t\right) \end{bmatrix}^{\mathrm{T}},$$

$$T_{+2} = \mathrm{e}^{\mathrm{Im}(\omega_{+2})t}\begin{bmatrix} -\cos\left(kx-\mathrm{Re}\left(\omega_{+2}\right)t\right)-\cos\left(kx+\mathrm{Re}\left(\omega_{+2}\right)t\right), \\ \cos\left(kx+\alpha-\mathrm{Re}\left(\omega_{+2}\right)t\right)-\cos\left(kx+\alpha+\mathrm{Re}\left(\omega_{+2}\right)t\right), \\ -\cos\left(kx-\alpha-\mathrm{Re}\left(\omega_{+2}\right)t\right)-\cos\left(kx-\alpha+\mathrm{Re}\left(\omega_{+2}\right)t\right), \\ \cos\left(kx-\mathrm{Re}\left(\omega_{+2}\right)t\right)+\cos\left(kx+\mathrm{Re}\left(\omega_{+2}\right)t\right) \end{bmatrix}^{\mathrm{T}},$$

$$T_{-2} = \mathrm{e}^{\mathrm{Im}(\omega_{-2})t}\begin{bmatrix} -\cos\left(kx-\mathrm{Re}\left(\omega_{-2}\right)t\right)-\cos\left(kx+\mathrm{Re}\left(\omega_{-2}\right)t\right), \\ \cos\left(kx+\beta-\mathrm{Re}\left(\omega_{-2}\right)t\right)-\cos\left(kx+\beta+\mathrm{Re}\left(\omega_{-2}\right)t\right), \\ -\cos\left(kx-\beta-\mathrm{Re}\left(\omega_{-2}\right)t\right)-\cos\left(kx-\beta+\mathrm{Re}\left(\omega_{-2}\right)t\right), \\ \cos\left(kx-\mathrm{Re}\left(\omega_{-2}\right)t\right)+\cos\left(kx+\mathrm{Re}\left(\omega_{-2}\right)t\right) \end{bmatrix}^{\mathrm{T}},$$

$$\tan\alpha = \frac{\cosh\psi}{1+\sqrt{2-\cosh 2\psi}}, \qquad \tan\beta = \frac{\cosh\psi}{1-\sqrt{2-\cosh 2\psi}}. \tag{17}$$

Obviously, the temperature fields in the four channels are uneven with divergently evolving phase differences between adjacent channels.

4.2. Perturbation at high-order EP

A four-channel structure with high-order EP provides us more degrees of freedom to manipulate the temperature field. We have investigated how the perturbation impacts the APT system on the basis of high-order EP. Firstly, we assign all adjacent channels with opposite velocities at the high-order EP. Then, a perturbation Δv is added to the channels with different directions. The velocities of background motion in different channels are $v_{\rm EP1}-\Delta v$, $-v_{\rm EP1}-\Delta v$, $v_{\rm EP1}+\Delta v$, and $-v_{\rm EP1}+\Delta v$, respectively. The Hamiltonian containing this perturbation is[39]

$$H' = \begin{pmatrix} -\mathrm{i}S_0 - k\,(v_{\rm EP}-\Delta v) & \mathrm{i}h & 0 & 0 \\ \mathrm{i}h & -\mathrm{i}(S_0+h)+k(v_{\rm EP}+\Delta v) & \mathrm{i}h & 0 \\ 0 & \mathrm{i}h & -\mathrm{i}(S_0+h)-k(v_{\rm EP}+\Delta v) & \mathrm{i}h \\ 0 & 0 & \mathrm{i}h & -\mathrm{i}S_0+k(v_{\rm EP}-\Delta v) \end{pmatrix}. \tag{18}$$

By increasing the perturbation strength from zero, the initial high-order EP ($\Delta v = 0$) splits into two second-order EPs. Simulation results show that when the perturbation strength is between the two EPs at the lowest branch, the whole system is still in APT symmetric phase, which displays a strong anti-perturbation ability. After crossing this region, the phase differences of adjacent channels show periodic oscillations.

5. Conclusion and perspectives

In this paper, we give a short review on the APT symmetry and the phase transition at EP in diffusive systems (or thermal systems). First, we discuss the realization of APT symmetry in a double-channel diffusive system. Then, we analyze the phase transition of temperature profiles around the EP. Finally, we extend the double-channel toy model to a four-channel one for the exploration of high-order EP and various wavelike motion of heat flow. In a general conclusion, the phase difference of adjacent channels is always static, when the introduced flow velocity is below $v_{\rm EP}$ or in the APT symmetry phase. Above $v_{\rm EP}$ or in the APT symmetry broken phase, the phase begins to dynamically evolve in time. The APT symmetry in non-Hermitian diffusive systems provides us a unique platform to investigate the heat flow manipulation in a different way, such as thermal stealing, heat rotation and concentration,[44] or even topological non-Hermitian bulk-boundary state.[45–47]

References

[1] Kato T 1966 *Perturbation Theory of Linear Operators* (Berlin: Springer)

[2] Bender C M and Boettcher S 1998 *Phys. Rev. Lett.* **80** 5243

[3] Lévai G and Znojil M 2000 *J. Phys. Math. Gen.* **33** 7165

[4] Ahmed Z 2011 *Phys. Lett. A* **282** 343

[5] El-Ganainy R, Makris K G, Christodoulides D N and Musslimani Z H 2007 *Opt. Lett.* **32** 2632

[6] Lin Z, Ramezani H, Eichelkraut T, *et al.* 2011 *Phys. Rev. Lett.* **106** 213901

[7] Zhu X, Ramezani H, Shi C, Zhu J and Zhang X 2014 *Phys. Rev. X* **4** 031042
[8] Zhu X, Feng L, Zhang P, Yin X and Zhang X 2013 *Opt. Lett.* **38** 002821
[9] Feng L, Xu Y Long, Fegadolli W, *et al.* 2013 *Nat. Mater* **12** 108
[10] Cao P, Yang X, Wang S, *et al.* 2017 *IEEE Photonics Journal* **9** 2200209
[11] Wong Z J, Xu Y L, Kim J, *et al.* 2016 *Nat. Photonics* **10** 796
[12] Peng B, Özdemirş K, Rotter S, *et al.* 2014 *Science* **346** 328
[13] Chong Y D, Li G and Stone A D 2011 *Phys. Rev. Lett.* **106** 093902
[14] Chen W, Özdemirş K, Zhao G, *et al.* 2017 *Nature* **548** 192
[15] Wiersig J 2014 *Phys. Rev. Lett.* **112** 203901
[16] Fang Y, Li X, Xia J and Xu Z 2019 *IEEE Sensors Journal* **19** 2533
[17] Doppler J, Mailybaev A A, Böhm J, *et al.* 2016 *Nature* **537** 76
[18] Liu Q, Li S, Wang B, *et al.* 2020 *Phys. Rev. Lett.* **124** 153903
[19] Ke S, Zhao D, Fu J, *et al.* 2020 *IEEE J. Sel. Top Quant.* **26** 4401008
[20] Borgnia D S, Kruchkov A J and Slager R J 2020 *Phys. Rev. Lett.* **124** 056802
[21] Gong Z, Ashida Y, Kawabata K, *et al.* 2018 *Phys. Rev. X* **8** 031079
[22] Li G and Tureci H E 2013 *Phys. Rev. A* **88** 053810
[23] Wu J, Artoni M and Rocca G 2014 *Phys. Rev. Lett.* **113** 123004
[24] Peng P, Cao W, Shen C, *et al.* 2016 *Nature Phys* **12** 1139
[25] Antonosyan D A, Solntsev A S and Sukhorukov A A 2015 *Opt. Lett.* **40** 4575
[26] Yang F, Liu Y C and You L 2017 *Phys. Rev. A* **96** 053845
[27] Choi Y, Hahn C, Yoon J W and Song S H 2018 *Nat. Commun.* **9** 2182
[28] Zhang X L, Jiang T S and Chan C T 2019 *Light: Sci. & Appl.* **8** 88
[29] Li Y, Peng Y, Han L, *et al.* 2019 *Science* **364** 170
[30] Fan C Z, Gao Y and Huang J P 2008 *Appl. Phys. Lett.* **92** 251907
[31] Narayana S and Sato Y 2012 *Phys. Rev. Lett.* **108** 214303
[32] Han T, Bai X, Gao D, Thong J, Li B and Qiu C W 2014 *Phys. Rev. Lett.* **112** 054302
[33] Li J, Li Y, Cao P, *et al.* 2020 *Adv. Mater.* **32** 2003823
[34] Schittny R, Kadic M, Guenneau S and Wegener M 2013 *Phys. Rev. Lett.* **110** 195901
[35] Peng Y G, Li Y, Cao P C, *et al.* 2020 *Adv. Funct. Mater.* **30** 2002061
[36] Hu R, Zhou S, Li Y, *et al.* 2018 *Adv. Mater.* **3** 1707237
[37] Li Y, Zhu K J, Peng Y G, *et al.* 2019 *Nat. Mater.* **18** 48
[38] Moccia M, Castaldi G, S Savo, Sato Y and Galdi V 2014 *Phys. Rev. X* **4** 021025
[39] Cao P, Li Y, Peng Y, *et al.* 2020 *ES Energy & Environment* **7** 48
[40] KÖzdemir S, Rotter S, Nori F, *et al.* 2019 *Nat. Mater.* **18** 783
[41] Miri M A and Alù A 2019 *Science* **363** eaar7709
[42] Bejan A 2013 *Convection Heat Transfer*, 4th edn. (New York: Wiley)
[43] Xu L and Huang J 2020 *Chin. Phys. Lett.* **37** 080502
[44] Xu L and Huang J 2020 *Int J Heat Mass Tran* **159** 120133
[45] Yoshida T and Hatsugai Y 2020 arXiv: 2007.08730
[46] Liu J, Han Y and Liu C 2020 *Chin. Phys. B* **29** 010302
[47] Liu J, Han Y and Liu C 2019 *Chin. Phys. B* **28** 100304